European Review for Medical and Pharmacological Sciences 2020; 24: 2505-2517

Knockdown of lncRNA XIST inhibits hypoxia-induced glycolysis, migration and invasion through regulating miR-381-3p/NEK5 axis in nasopharyngeal carcinoma

C.-H. ZHAO, X.-F. BAI, X.-H. HU

Department of Otorhinolaryngology, the First People's Hospital of Tongxiang City, Tongxiang, P.R. China

C.-H. Zhao and *X.-F. Bai* contributed to this work equally

Abstract. – OBJECTIVE: Hypoxia is an important feature of nasopharyngeal carcinoma (NPC). Growing evidence demonstrated that long non-coding RNAs (lncRNAs) could participate in cancer progression and hypoxia regulation. However, the exact roles and underlying mechanism of lncRNA X-inactive specific transcript (XIST) in NPC under hypoxia are still unclear.

MATERIALS AND METHODS: The expressions of XIST, microRNA-381-3p (miR-381-3p) and NIMA related kinase 5 (NEK5) were detected by quantitative Real-time polymerase chain reaction (qRT-PCR). The glucose consumption and lactate production were measured using the glucose assay kit and lactate assay kit, respectively. Western blot assay was used to determine the protein levels of hexokinase II (HK2) and NEK5. Transwell assay was employed to evaluate cell migration and invasion. The interaction between miR-381-3p and XIST or NEK5 was predicted by bioinformatics analysis and verified by dual-luciferase reporter assay. The mice xenograft model was established to investigate the roles of XIST in NPC progression *in vivo*.

RESULTS: XIST and NEK5 were highly expressed while miR-381-3p was lowly expressed in NPC (tissues and cells) and hypoxia-induced NPC cells. Deficiency of XIST or NEK5 suppressed hypoxia-induced glycolysis and metastasis in NPC cells. Moreover, miR-381-3p could directly bind to XIST and its inhibition reversed the inhibitory effects of XIST knockdown on glycolysis and metastasis under hypoxia. NEK5 was a direct target of miR-381-3p and its interference attenuated the promotive effects of miR-381-3p downregulation on glycolysis and metastasis under hypoxic conditions. Besides, interference of XIST decreased tumor growth by upregulating miR-381-3p and downregulating NEK5.

CONCLUSIONS: XIST knockdown inhibited glycolysis and metastasis in hypoxia-induced NPC cells through regulating miR-381-3p/NEK5 axis, providing new insights into the pathogenesis of NPC.

Key Words:

Nasopharyngeal carcinoma, Hypoxia, XIST, MiR-381-3p, NEK5, Glycolysis, Metastasis.

Introduction

Nasopharyngeal carcinoma (NPC) is the most frequent head and neck malignancy in Southern China and Southeast Asia[1,2]. In recent years, despite many treatments were used for NPC, including radiotherapy and chemotherapy, the prognosis for advanced NPC patients is still poor[3]. Hypoxia has been recognized as a typical feature of solid tumors, causing metabolic reprogramming from oxidative stress to glycolysis and enhancing the risk of tumor metastasis and death[4-6]. Under hypoxic condition, cancer cells can use glycolysis as the main mechanism for adenosine triphosphate (ATP) production, and glycolysis contributes to cancer cell proliferation and survival[7]. Hence, it is critical to elucidate the molecular mechanisms of NPC under hypoxic condition.

Long non-coding RNAs (lncRNAs), a class of more than 200 nucleotides in length, lack protein-coding capacity and play regulatory roles in various physiopathology processes[8]. Moreover, lncRNAs have been regarded as potential therapeutic targets in NPC[9]. LncRNA ROR might act as a therapeutic target for NPC and promoted NPC progression[10]. Moreover, lncRNA EWSAT1 contributed to NPC cell growth *via* targeting miR-326/-330-5p[11]. Besides, previous studies demonstrated that lncRNA X-inactive specific transcript (XIST) acted as an oncogene in many tumors, including glioma, gastric cancer[12], hepatocellular carcinoma[13], non-small cell lung can-

Corresponding Author: Xiong-Hui Hu, MD; e-mail: umrfot@163.com

cer[14], and NPC[15], indicating that XIST played vital roles in the pathogenesis of cancers. However, whether XIST is related to glycolytic transformation and metastasis under hypoxia stress remains unknown.

LncRNAs function as competing endogenous RNAs (ceRNAs) to modulate gene expression by sponging microRNA (miRNA)[16]. MiRNAs, short non-coding RNA molecules (~ 22 nucleotides), modulate gene expression through binding to the 3'-untranslated region (3'UTR) of target mRNAs. Many miRNAs are dysregulated in diverse cancers and serve as oncogenes or tumor suppressors[17]. Among these miRNAs, miR-381-3p was dysregulated in several human cancer types, such as oral squamous cell carcinoma[18], cervical cancer[19], and thyroid carcinoma[20]. Nevertheless, the potential role and underlying mechanism for miR-381-3p in NPC have not been reported.

NIMA related kinase 5 (NEK5), a member of NEK kinases family, plays critical roles in cell differentiation, cell growth, cell apoptosis, and cell death[21,22]. NEK5 promoted proliferation of breast cancer cells by upregulating Cyclin A2[23]. To the best of our knowledge, there is no report on the effect of NEK5 on hypoxia-induced glycolysis and metastasis in NPC cells.

In the current research, we determined the levels of XIST, miR-381-3p, and NEK5 in NPC tissues and cells, and explored their functional effects on glycolysis and metastasis in NPC cells under hypoxia. Moreover, we investigated the relationships among XIST, miR-381-3p, and NEK5 in hypoxia-induced NPC cells. The aim of our research was to provide a new perspective on the diagnosis and treatment of NPC.

Materials and Methods

Clinical Samples

In this study, 25 pairs of NPC tissues and adjacent normal samples were collected from patients undergoing surgery at The Affiliated Yantai Yuhuangding Hospital of Qingdao University. These patients did not receive chemotherapy, radiotherapy or other therapy before surgery. Excised fresh tissues were promptly frozen in liquid nitrogen and then kept at -80°C until the experiments were performed. Before using these tissues, each patient has signed informed consent. This research was approved by Research Ethics Committee of The Affiliated Yantai Yuhuangding Hospital of Qingdao University.

Cell Culture and Transfection

NPC cell lines (HK-1 and C666-1) and nasopharyngeal epithelial cell line (NP69) were bought from BeNa Culture Collection (Beijing, China) and cultured in Roswell Park Memorial Institute-1640 (RPMI-1640) medium (Gibco, Grand Island, NY, USA) supplemented with fetal bovine serum (FBS; 10%) (Gibco), penicillin (100 U/mL) and streptomycin (100 μg/mL) (Gibco) in a moist incubator with CO_2 (5 %) at 37°C. For hypoxia treatment, cells were placed in a hypoxia chamber with 1% oxygen O_2, 5% CO_2 and 94% N_2 gas mixture.

The small interfering RNA against XIST or XIST (si-XIST or si-NEK5) and their negative control (si-NC), miR-381-3p mimic (miR-381-3p) and its negative control (miR-NC), miR-381-3p inhibitor (anti-miR-381-3p) and its negative control (anti-miR-NC) were provided by RiboBio (Guangzhou, China). Lentivirus-mediated shRNA interference targeting XIST (sh-XIST) and its negative control (sh-NC) were constructed by GeneCopoeia (Rockville, MD, USA). Cell transfection was conducted using Lipofectamine 3000 (Invitrogen, Carlsbad, CA, USA).

Quantitative Real-Time Polymerase Chain Reaction (qRT-PCR)

Under the commendations of instructions, total RNA was extracted from tissues and cell lines using TRIzol Reagent (Invitrogen). Complementary DNA (cDNA) was then synthesized using the Prime-Script RT Reagent Kit (TaKaRa, Otsu, Shiga, Japan). The qRT-PCR reactions were carried out on ABI 7500 Fast Real-Time PCR system (Applied Biosystems, Foster City, CA, USA) using the SYBR Green Master Mix (Applied Biosystems). The expression of genes was evaluated with $2^{-\Delta\Delta Ct}$ method and normalized to glyceraldehyde-3-phosphate dehydrogenase (GAPDH) or U6. In this study, primers used for qRT-PCR were listed as below: XIST (Forward, 5'-CCTCTCCACATACCTCAGT-3'; Reverse, 5'-ACATAATCACACGCATACCA-3'), miR-381-3p (Forward, 5'-TAATCTGACTATACAAGGGCAAGCT-3'; Reverse, 5'-TATGGTTGTTCTGCTCTCTGTCTC-3'), NEK5 (Forward, 5'-GGAAGAACAAAATGAAGGACCA-3'; Reverse, 5'-CTTCATGTCGTTGTGGTACTGTT-3'), GAPDH (Forward, 5'-CGCTCTCTGCTCCTCCTGTTC-3'; Reverse, 5'- ATCCGTTGACTCCGACCTTCAC-3'), U6 (Forward, 5'-GCTTCGGCAGCACATATACTAAAAT-3'; Reverse, 5'- CGCTTCACGAATTTGCGTGTCAT-3').

Detection of Glucose and Lactate Levels

Glucose assay kit (Sigma-Aldrich, St. Louis, MO, USA) was employed to detect the glucose consumption and lactate assay kit (BioVision, Mountain View, CA, USA) was utilized to measure the lactate production. Finally, the glucose consumption or lactate production was determined using a standard calibration curve and normalized to total protein.

Western Blot Analysis

After treatment/transfection, RIPA lysis buffer (Beyotime, Shanghai, China) containing phenylmethylsulphonyi fluoride (PMSF; Beyotime) was used to extract total protein. Subsequently, BCA Protein Assay Kit (Beyotime) was applied to determine the protein concentration of each sample. Protein samples (about 40 μg) were separated using sodium dodecyl sulfate-polyacrylamide gel electrophoresis (SDS-PAGE), followed by transferring onto polyvinylidene difluoride (PVDF) membranes (0.2 μm, Beyotime). After that, membranes were blocked in 5% non-fat milk and then probed with specific primary antibody against Hexokinase II (HK2) (1:5000, ab227198, Abcam, Cambridge, UK), NEK5 (1: 500; sc-515757, Santa Cruz Biotechnology, Santa Cruz, CA, USA), or β-Actin (1:2000, ab8227, Abcam) at 4°C for 12-16 h. Then, membranes were incubated with horseradish peroxidase (HRP)-conjugated secondary antibody. Enhanced chemiluminescence (ECL) reagent (Tanon, Shanghai, China) was employed to examine protein bands. ImageJ software was applied to evaluate the bands density. β-Actin served as the internal control.

Transwell Assay

For migration assay, HK-1 and C666-1 cells (100 μL, 2×10^4 cells/well) were placed in the upper chamber of each insert (8 μm pores, Corning Incorporated, Corning, NY, USA) with a non-coated membrane. For invasion assay, HK-1 and C666-1 cells (100 μL, 2×10^4 cells/well) were placed in the top chamber with Matrigel (Becton Dickinson, Brea, CA, USA). The medium (RPMI-1640, 600 μL) containing 10% FBS was put into the lower chambers. Then, cells were scraped out of the top chamber using a cotton swab following incubation for 24 h, and the cells that had migrated and invaded through the pore were fixed using paraformaldehyde (4%, 20 min) and stained using the crystal violet (0.1%, 1 h). Lastly, migrated and invaded cells were photographed and counted using a microscope (Leica, Wetzlar, Germany).

Dual-Luciferase Reporter Assay

Bioinformatics analysis was performed using starBase v2.0 or TargetScan. The XIST or NEK5 3'UTR sequences containing wild-type (WT) or mutant (MUT) binding sites of miR-381-3p were cloned into downstream of pmirGlO luciferase reporter vector (Promega, Madison, WI, USA) to construct WT (WT-XIST, WT-NEK5) luciferase reporter vectors or MUT (MUT-XIST, MUT-NEK5) luciferase reporter vectors. Cells were co-transfected with luciferase vector and miR-381-3p (or miR-NC) for 48 h. Finally, dual-luciferase reporter assay system (Promega, Madison, WI, USA) was utilized to assess the luciferase activity, followed by normalizing to Renilla luciferase activity.

Tumor Xenograft Model

The sh-XIST or sh-NC was transfected into HK-1 cells. Stably transfected cells (1×10^6) were inoculated subcutaneously in BALB/c nude mice (n=5 per group, female, six-week-old, Shanghai Experimental Animal Center, Shanghai, China). The animal experiments were approved by the Animal Care and Use Committee of The Affiliated Yantai Yuhuangding Hospital of Qingdao University. From the 1th week, tumor volume was examined using a caliper every week, and calculated following the equation: volume = length × width^2 ×0.5. These mice were euthanized after injection for 4 weeks, and tumor specimens were weighed and collected for further analysis.

Statistical Analysis

In our research, statistical analyses were performed using Graph Prism 6.0 software (GraphPad Prism, San Diego, CA, USA). Data were displayed as the mean ± standard deviation (SD) from at least three independent experiments. Statistical comparisons were analyzed with the Student's *t*-test (for two groups) and a one-way analysis of variance (ANOVA; for more than two groups) followed by Tukey's post-hoc test. Spearman rank correlation was employed to investigate the correlations between miR-381-3p and XIST or NEK5. $p<0.05$ was considered statistically significant.

Results

XIST Was Upregulated in NPC Tissues and Cells, and Hypoxia Promoted XIST Expression in NPC Cells

Firstly, we measured the expression of XIST in NPC tissues and cells by qRT-PCR. The re-

sults showed that XIST abundance was markedly increased in NPC tissues compared with that in adjacent normal tissues (Figure 1A). Similarly, the expression of XIST was also enhanced in NPC cell lines (HK-1 and C666-1) relative to nasopharyngeal epithelial cell line (NP69) (Figure 1B). To explore whether hypoxia influences XIST expression in NPC, HK-1 and C666-1 cells were exposed at various times (0 h, 3 h, 6 h, 12 h, 24 h and 48 h) in a hypoxic incubator with 1% O_2. As displayed in Figure 1C and 1D, hypoxia resulted in an increase of XIST level in a time-dependent manner. These results suggested that hypoxia induced XIST expression in NPC cells.

Knockdown of XIST Suppressed Hypoxia-Induced Glycolysis, Migration and Invasion in NPC Cells

Both tumor hypoxia and dysregulated metabolism are typical features of cancer[24]. To investigate whether XIST was involved in the metabolic response to hypoxia in NPC cells, HK-1 and C666-1 cells were transfected with si-NC or si-XIST and then cultured in a hypoxic incubator with 1% O_2. The transfection efficiency was examined using qRT-PCR. Results showed that the expression of XIST was evidently decreased in HK-1 and C666-1 cells transfected with si-XIST under hypoxic condition (Figure 2A), suggesting the successful introduction of si-XIST into HK-1 and C666-1 cells. Moreover, we found that hypoxic obviously enhanced the glucose consumption and lactate production in HK-1 and C666-1 cells, while these effects were abated by downregulating XIST (Figure 2B and 2C). HK2 was identified as a key rate-limiting enzyme in glucose metabolism, which catalyzes the reaction of the first step of glycolysis, playing an essential role in cancer glucose metabolism[25]. Western blot assay demonstrated that the protein level of HK2 was increased under hypoxic condition, which was

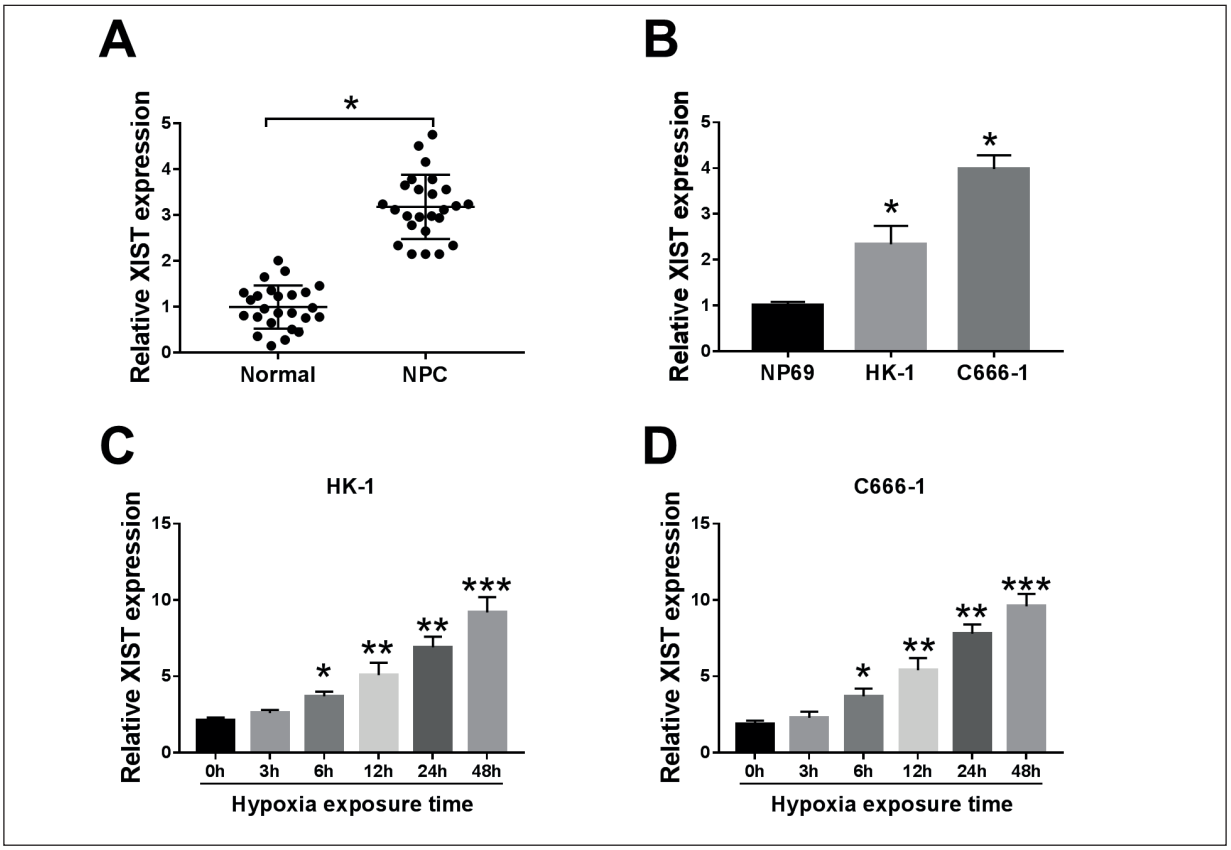

Figure 1. XIST was upregulated in NPC and hypoxia enhanced XIST expression in NPC cells. **A**, The expression of XIST was detected by qRT-PCR in 25 pairs of NPC tissues and adjacent normal tissues. **B**, The abundance of XIST was measured by qRT-PCR in NPC cell lines (HK-1 and C666-1) and nasopharyngeal epithelial cell line (NP69). **C-D**, HK-1 and C666-1 cells were exposed at different times (0 h, 3 h, 6 h, 12 h, 24 h and 48 h) in a hypoxic incubator with 1% O_2, and then XIST level was assessed using the qRT-PCR analysis. *p<0.05, **p<0.01, ***p<0.001.

reversed by knockdown of XIST in HK-1 and C666-1 cells (Figure 2D). Furthermore, we investigated the functional effects of hypoxia and XIST on metastasis in NPC cells. As shown in Figure 2E and 2F, the number of migrated and invaded cells was significantly enhanced under hypoxic condition, which would be abolished by silencing XIST. All these findings suggested that deficiency of XIST suppressed hypoxia-induced glycolysis and metastasis in NPC cells.

MiR-381-3p Was a Direct Target of XIST, and Was Downregulated in NPC and Hypoxia-Induced NPC Cells

It is well known that lncRNAs can exert their functions through binding with their downstream miRNAs[26]. To search the downstream target of XIST, starBase v2.0 was performed. As presented in Figure 3A, miR-381-3p was predicted as a direct target of XIST. Subsequently, the prediction was confirmed through dual-luciferase reporter assay. Results indicated that overexpression of miR-381-3p greatly reduced the luciferase activity of WT-XIST in HK-1 and C666-1 cells, whereas miR-381-3p upregulation had no impact on the luciferase activity of MUT-XIST (Figure 3B). Next, we studied the effect of XIST on miR-381-3p expression. The qRT-PCR analysis demonstrated that interference of XIST promoted the expression of miR-381-3p in HK-1 and C666-1 cells (Figure 3C). Moreover, we observed that the expression of miR-381-3p was

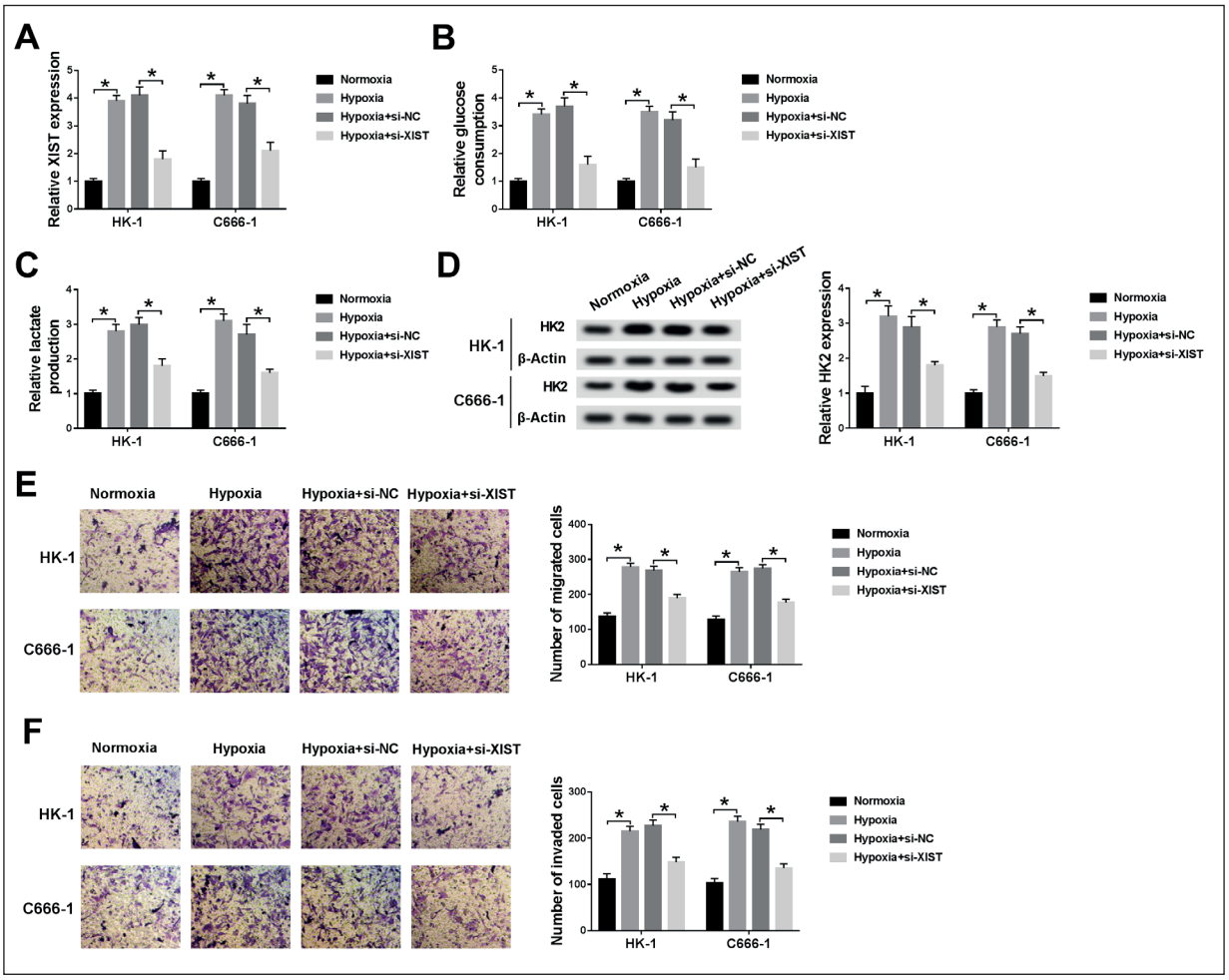

Figure 2. Interference of XIST repressed hypoxia-induced glycolysis and metastasis in NPC cells. HK-1 and C666-1 cells were cultured in a 21% O_2 normoxic or 1% O_2 hypoxic incubator for 24 h, or cells were transfected with si-NC or si-XIST before hypoxic treatment. **A**, The expression of XIST determined by qRT-PCR. **B**, Glucose consumption was measured by a glucose assay kit. **C**, Lactate production was assessed using a lactate assay kit. **D**, The protein expression of HK2 was analyzed by Western blot assay. **E-F**, Transwell assay was employed to assess the migration and invasion abilities (100×). *p<0.05.

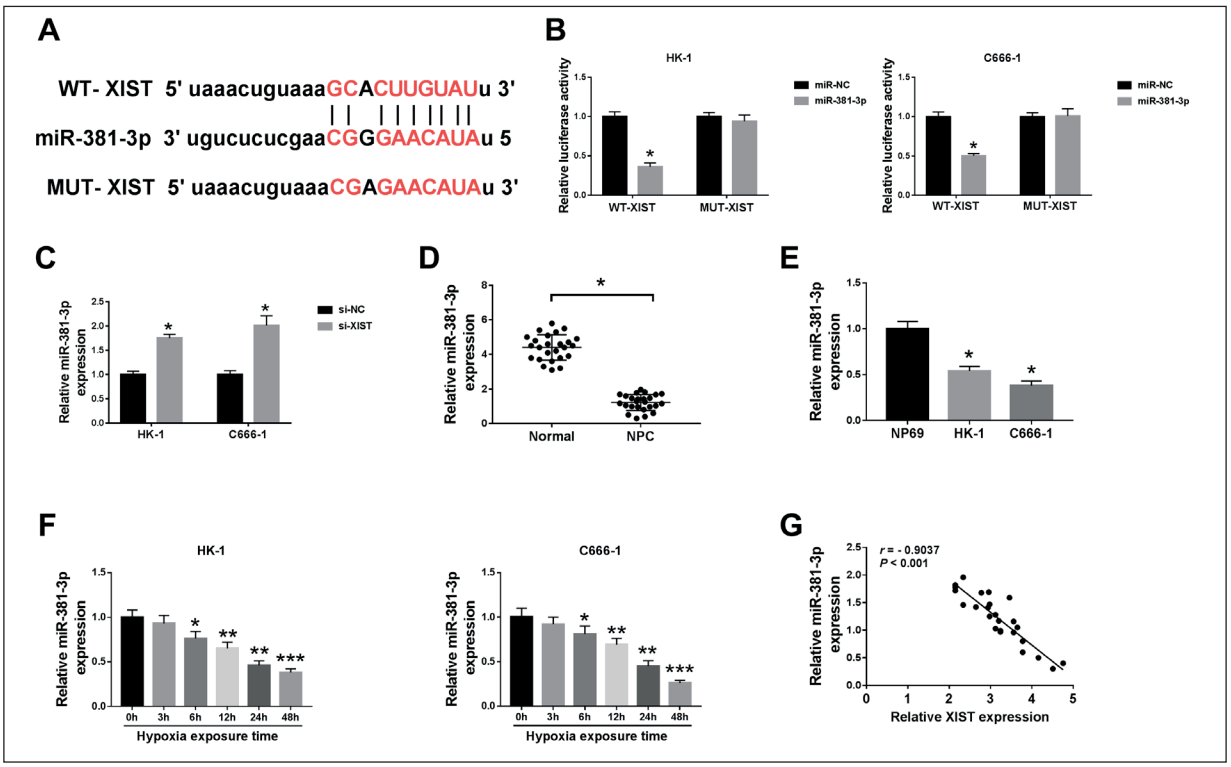

Figure 3. MiR-381-3p was a direct target of XIST and decreased in NPC and hypoxia-induced NPC cells. **A**, The potential binding sites of miR-381-3p and XIST were predicted by starBase v2.0. **B**, HK-1 and C666-1 cells were co-transfected with WT-XIST or MUT-XIST and miR-381-3p or miR-NC, and then relative luciferase activity was measured. **C**, The miR-381-3p expression was determined in HK-1 and C666-1 cells transfected with si-NC or si-XIST by qRT-PCR. **D**, The level of miR-381-3p was measured by qRT-PCR in 25 pairs of NPC tissues and adjacent normal tissues. **E**, The expression of miR-381-3p was assessed by qRT-PCR in NPC cell lines (HK-1 and C666-1) and nasopharyngeal epithelial cell line (NP69). **F**, The abundance of miR-381-3p level was evaluated using the qRT-PCR in HK-1 and C666-1 cells treated with hypoxia for various times (0 h, 3 h, 6 h, 12 h, 24 h and 48 h). **G**, The association between miR-381-3p level and XIST abundance was measured in NPC tissues. *p<0.05, **p<0.01, ***p<0.001.

decreased in NPC tissues and cells (Figure 3D and 3E). Furthermore, we found that hypoxic time-dependently inhibited miR-381-3p expression in HK-1 and C666-1 cells (Figure 3F). Besides, miR-381-3p expression was negatively correlated with XIST level in NPC tissues (r=-0.9037, p<0.001) (Figure 3G). Taken together, these data indicated that XIST could target to miR-381-3p in NPC cells.

Downregulation of miR-381-3p Promoted Hypoxia-Induced Glycolysis, Migration and Invasion, and Reversed the Inhibitory Function of XIST Deficiency

To further explore the relationship between miR-381-3p and XIST in hypoxia-induced NPC cells, loss-of-function experiments were carried out by transfection of anti-miR-381-3p or si-XIST + anti-miR-381-3p before hypoxic treatment. Results showed that the expression of miR-381-3p was reduced in HK-1 and C666-1 cells transfected with anti-miR-381-3p compared with in anti-miR-NC group (Figure 4A). Moreover, knockdown of miR-381-3p increased the glucose consumption, lactate production and HK2 expression in hypoxia-induced HK-1 and C666-1 cells and could reverse the inhibitory effects of XIST inhibition on glycolysis (Figure 4B-4D). Besides, we found that silencing miR-381-3p promoted cell migration and invasion in hypoxia-induced HK-1 and C666-1 cells, and also attenuated the suppressive impacts of XIST knockdown on migration and invasion (Figure 4E and 4F). Based on all above, we speculated that XIST knockdown inhibited hypoxia-induced glycolysis and metastasis by upregulating miR-381-3p in NPC cells.

NEK5 Was a Downstream Target of miR-381-3p in NPC Cells

MiRNAs have been suggested to exert their biological function through modulating their target mRNAs [27]. TargetScan was used to predict the targets of miR-381-3p, and we found that miR-381-3p might bind to 3'UTR of NEK5 mRNA (Figure 5A). Next, the prediction was confirmed by dual-luciferase reporter assay. Results showed that after transfection of miR-381-3p mimic, the luciferase activity of WT-NEK5 was decreased, while the luciferase activity of MUT-NEK5 was almost not changed in HK-1 and C666-1 cells (Figure 5B). Next, the mRNA and protein expression of NEK5 were examined in NEK5- or miR-381-3p-downregulated NPC cells. The qRT-PCR and Western blot results proved that the expression of NEK5 was reduced in HK-1 and C666-1 cells transfected with si-NEK5, while deficiency of miR-381-3p increased the expression of NEK5 (Figure 5C and 5D). Collectively, we confirmed that NEK5 was a direct target of miR-381-3p and was negatively regulated by miR-381-3p in NPC cells.

NEK5 Level Was Enhanced in NPC Tissues and Cells, and Hypoxia Promoted NEK5 Expression in NPC Cells

According to the results of qRT-PCR and Western blot, we uncovered that the mRNA and protein expression of NEK5 were upregulated in NPC tissues and cells (Figure 6A-6D). Moreover, hypoxia led to increase of NEK5 mRNA and protein expression levels in HK-1 and C666-1 cells in a time-dependent manner (Figure 6E and 6F). Besides, we observed that the NEK5 mRNA level was negatively correlated with miR-381-3p abundance in NPC tissues

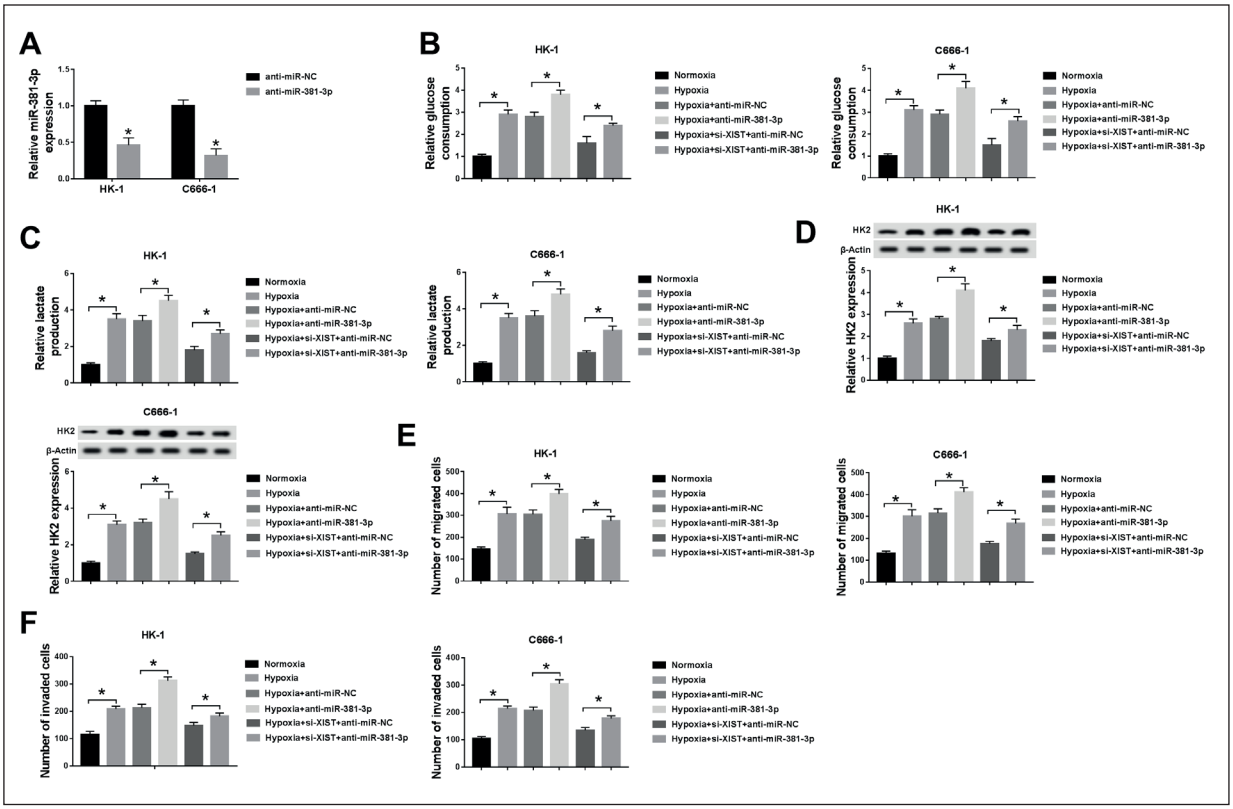

Figure 4. Knockdown of miR-381-3p reversed the inhibitory effects of XIST interference on glycolysis and metastasis in hypoxia-induced NPC cells. **A**, The expression of miR-381-3p was determined by qRT-PCR in HK-1 and C666-1 cells transfected with anti-miR-NC or anti-miR-381-3p. **B-F,** HK-1 and C666-1 cells were cultured in hypoxic or normoxic condition, or cells were transfected with anti-miR-NC, anti-miR-381-3p, si-XIST + anti-miR-NC, or si-XIST + anti-miR-381-3p prior to hypoxic exposure. **B-C**, Glucose consumption or lactate production was measured by glucose assay kit or lactate assay kit, respectively. **D**, Western blot was performed to analyze the protein level of HK2. **E-F**, The number of migrated and invaded cells was determined by transwell assay. *$p<0.05$.

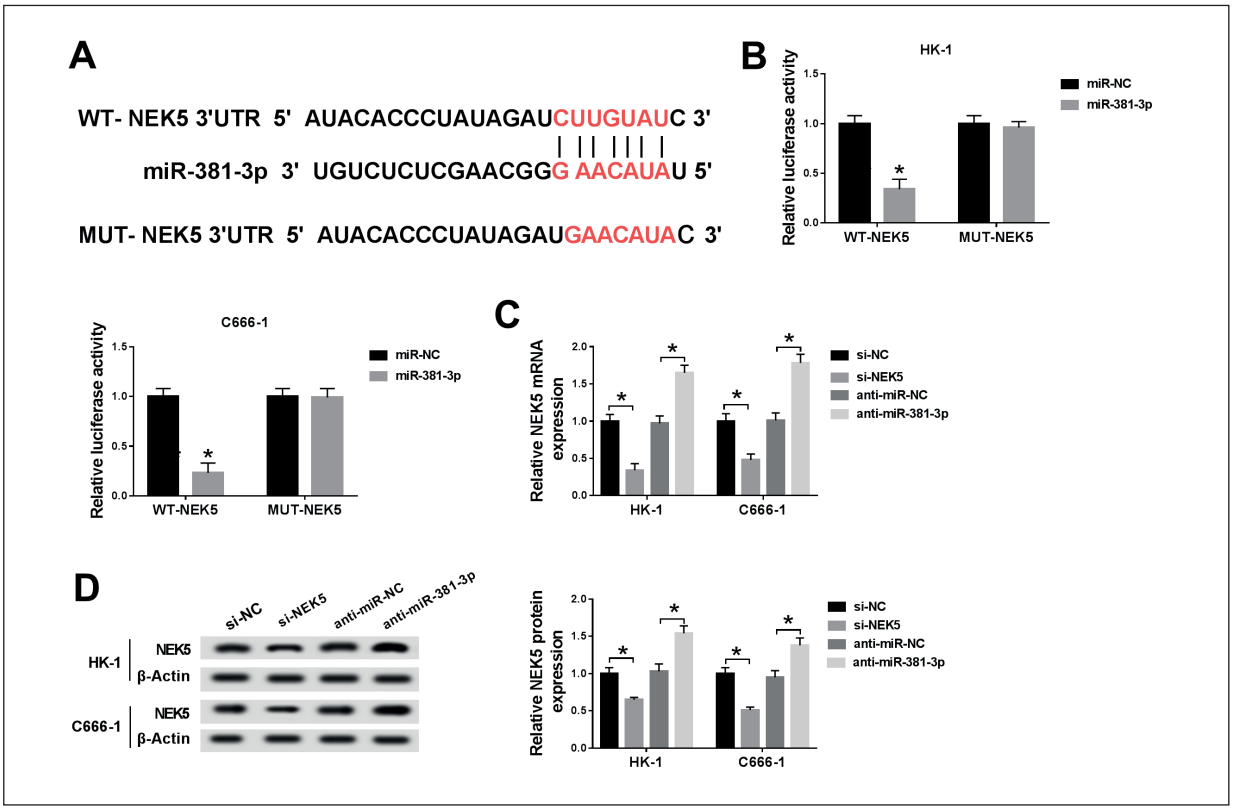

Figure 5. NEK5 was a downstream of miR-381-3p and was regulated by miR-381-3p. **A**, The putative binding sites between miR-381-3p and NEK5 were predicted by TargetScan. **B**, Relative luciferase activity was determined in HK-1 and C666-1 cells co-transfected with WT-NEK5 or MUT-NEK5 and miR-381-3p or miR-NC. **C**-**D**, The mRNA or protein expression of NEK5 was evaluated by qRT-PCR or Western blot analysis in HK-1 and C666-1 cells transfected with si-NC, si-NEK5, anti-miR-NC, or anti-miR-381-3p. *p<0.05.

(r=-0.8946, p<0.0001) (Figure 6G). Thus, these findings demonstrated that hypoxia induced NEK5 expression in NPC cells and might act as an oncogene in NPC.

Interference of NEK5 Suppressed Hypoxia-Induced Glycolysis, Migration and Invasion, and Could Reverse the Promotive Effects of miR-381-3p Knockdown

To further explore the effects of NEK5 and miR-381-3p on glycolysis and metastasis, HK-1 and C666-1 cells were transfected with si-NC, si-NEK5, anti-miR-381-3p + si-NC, or anti-miR-381-3p + si-NEK5 and then cultured in a hypoxic incubator with 1% O_2. As shown in Figure 7A-7C, inhibition of NEK5 suppressed hypoxia-induced glucose consumption, lactate production and HK2 expression, and the promotive effect of miR-381-3p deficiency on glycolysis was reversed by silencing NEK5 in HK-1 and C666-1 cells. Moreover, knockdown of NEK5 limited migration and invasion in hypoxia-induced HK-1 and C666-1 cells, and also partially abated the promotive impacts of miR-381-3p inhibition on migration and invasion (Figure 7D and 7E). These data indicated that inhibition of miR-381-3p promoted hypoxia-induced glycolysis and metastasis by upregulating NEK5 in NPC cells.

XIST Regulated NEK5 Expression via Sponging miR-381-3p in Vitro and in Vivo

To probe whether XIST functioned as a ceRNA to regulate NEK5 expression by sponging miR-381-3p, HK-1 and C666-1 cells were transfected with si-NC, si-XIST, si-XIST + anti-miR-NC, or si-XIST + anti-miR-381-3p. Results showed that the mRNA and protein expression levels of NEK5 were lowly expressed in si-XIST cells compared with si-NC cells, whereas the effect was abrogated by knockdown of miR-381-3p (Figure 8A and 8B). To explore whether the level of XIST expression influenced tumorigenesis, HK-1 cells transfected with the sh-XIST or si-NC were in-

troduced into nude mice. Knockdown of XIST decreased tumor volume and weight in sh-XIST group compared with si-NC group (Figure 8C and 8D). Next, the expression of XIST, miR-381-3p and NEK5 was analyzed in tumor tissues. As expected, knockdown of XIST reduced the expression levels of XIST and NEK5 in tumor tissues, while increased the miR-381-3p expression (Figure 8E-8G). Western blot analysis demonstrated that interference of XIST increased the protein level of NEK5 in tumor tissues (Figure 8H). To sum up, these results indicated that XIST acted as a molecular sponge of miR-381-3p to modulate NEK5 expression.

Discussion

Hypoxia is one of the crucial features of cancer and promoted glycolysis for ATP production[28]. It is

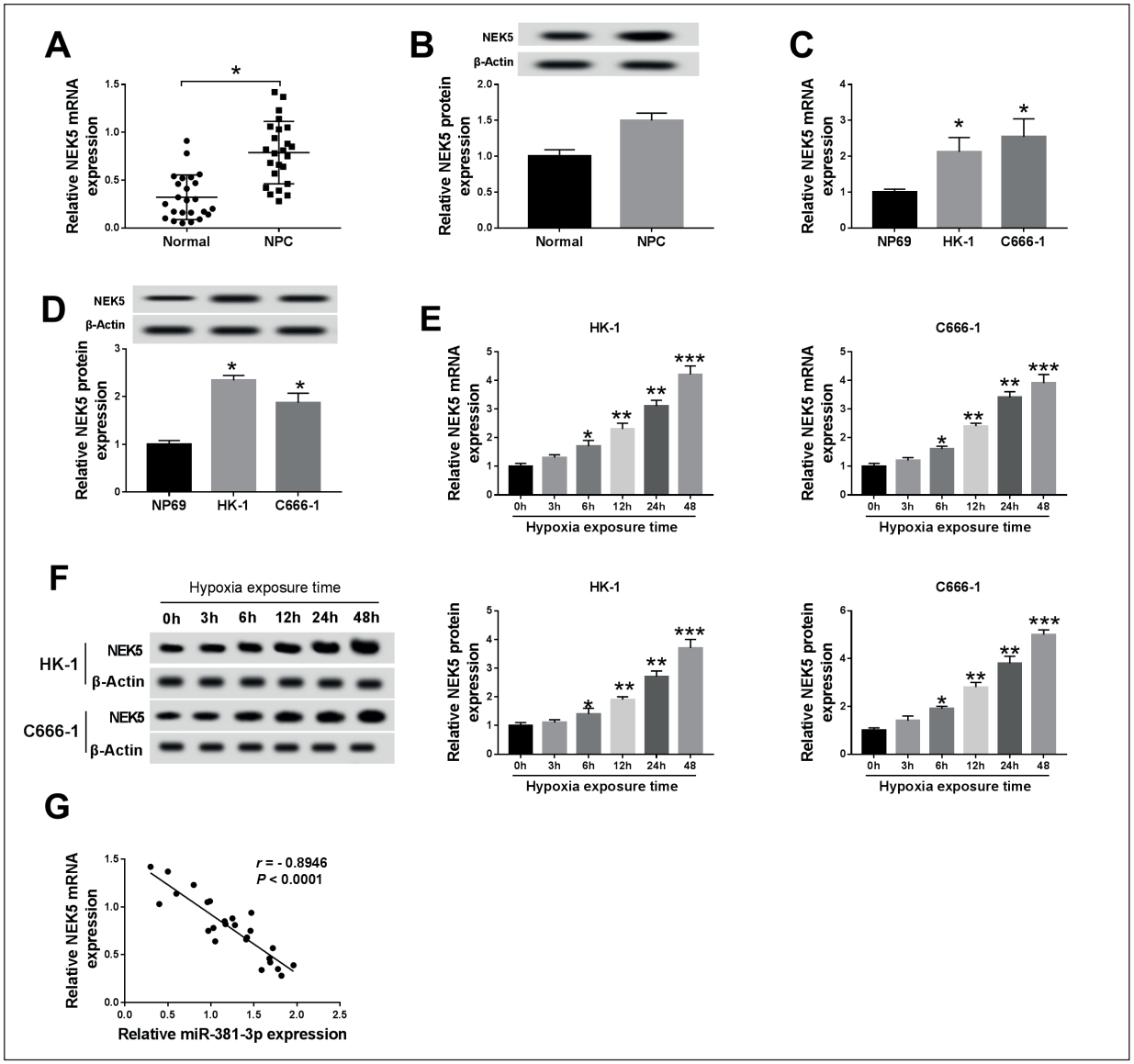

Figure 6. NEK5 was upregulated in NPC and hypoxia increased NEK5 expression in NPC cells. **A**-**B**, The mRNA and protein expression of NEK5 were measured in NPC tissues and adjacent normal tissues. **C**-**D**, The mRNA and protein expression of NEK5 were detected in NPC cell lines (HK-1 and C666-1) and nasopharyngeal epithelial cell line (NP69). **E**-**F**, NEK5 mRNA and protein expression were analyzed in HK-1 and C666-1 cells treated with hypoxia for different times (0 h, 3 h, 6 h, 12 h, 24 h and 48 h). **G**, The correlation between NEK5 mRNA level and miR-381-3p expression was analyzed in NPC tissues. *p<0.05, **p<0.01, ***p<0.001.

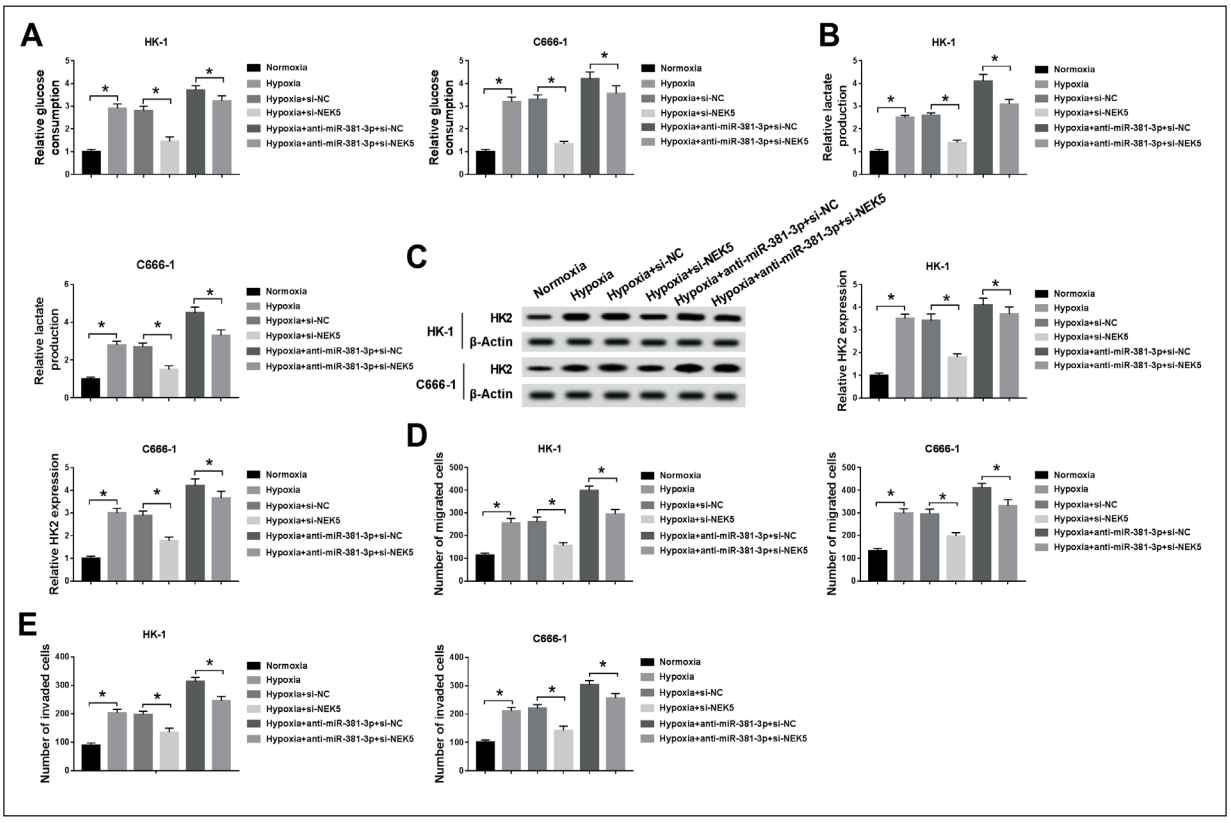

Figure 7. Deficiency of NEK5 partially abated the promotive effects of miR-381-3p knockdown on glycolysis and metastasis in hypoxia-induced NPC cells. HK-1 and C666-1 cells were cultured in normoxic or hypoxic condition for 24 h, or cells were transfected with si-NC, si-NEK5, anti-miR-381-3p + si-NC, or anti-miR-381-3p + si-NEK5 before treatment of hypoxia. **A**-**B**, Glucose consumption or lactate production was measured by glucose assay kit or lactate assay kit, respectively. **C**, Western blot assay was used to investigate the protein level of HK2. **D**-**E**, Transwell assay was used to assess the capacities of migration and invasion. *$p<0.05$.

increasingly recognized that lncRNAs are involved in the modulation of hypoxia [29]. Besides, dysregulation of lncRNAs has been proven to be tightly linked to the progression of NPC [30,31]. In this research, we first studied the impact of XIST on glycolysis and metastasis in NPC cells under hypoxia.

Growing amount of evidence demonstrated that XIST was identified as an oncogene in diverse tumors[32,33]. Besides, Song et al[34] pointed out that XIST was overexpressed in NPC tissues and accelerated NPC cell growth through targeting miR-34a-5p. Moreover, Cheng et al[35] reported that XIST abundance was obviously enhanced in NPC tissues and cells and its knockdown limited NPC cell progression as well as inhibited tumor growth *in vivo via* targeting miR-491-5p. Consistent with these results, we also proved that the XIST level was enhanced in NPC tissues and cell lines. Next, we explored the influence of hypoxia on XIST expression. As expected, we observed that the expression XIST was time-dependently increased after treatment of hypoxia. Under hypoxic condition, pyruvate catalyzed by lactate dehydrogenase A is converted into lactic acid to maintain anaerobic glycolysis[36]. Hypoxia could increase glycolysis in multiple human cancer cells, leading to the promotion of glucose consumption and lactate production[24,37]. Here, we demonstrated that glucose consumption, lactate production and HK2 protein expression were increased in hypoxia-induced NPC cells, suggesting that glycolysis was triggered. We also found that, under hypoxia condition, migration and invasion were promoted in NPC cells. Moreover, we uncovered that XIST knockdown decreased glycolysis, migration and invasion in NPC cells under hypoxia. Collectively, hypoxia facilitated glycolysis and metastasis through upregulating XIST expression in NPC cells.

LncRNAs usually execute their functional effects through serving as miRNAs inhibitors or sponges in different cancers[38,39]. Next, online software (starBase v2.0) was employed to predict the targeted miRNAs of XIST. Among these candidates, miR-381-3p was the focus of our research due to its anti-cancer role in multiple cancers. Besides, Yang et al[18] demonstrated that miR-381-3p suppressed the progression of oral squamous cell carcinoma cells *via* downregulation of FGFR2. Wu et al[40] stated that the accumulation of miR-381-3p could repress breast cancer cell growth, cell cycle progression and migration. However, there is no evidence in support of the effect of miR-381-3p in NPC and the interaction between XIST and miR-381-3p. Dual-luciferase reporter assay proved that XIST served as a molecular sponge of miR-381-3p. Additionally, data presented that miR-381-3p level was decreased in NPC tissues and cells, and its expression also decreased in NPC cells after exposure of hypoxia, implying that miR-381-3p might be involved in regulation of hypoxia. Next, we demonstrated that knockdown of miR-381-3p promoted hypoxia-induced glycolysis and metastasis, and could reverse anti-tumor role of XIST silence, suggesting that XIST regulated NPC progression by sponging miR-381-3p.

The biological effects of miRNAs are realized through modulating mRNA expression, so the possible targets for miR-381-3p should be probed in further analysis. TargetScan software showed that NEK5 might be a target of miR-381-3p, which was verified through the dual-luciferase reporter assay. NEK5 has been suggested to participate in cell cycle and cell apoptosis[41]. Prosser et al[23] man-

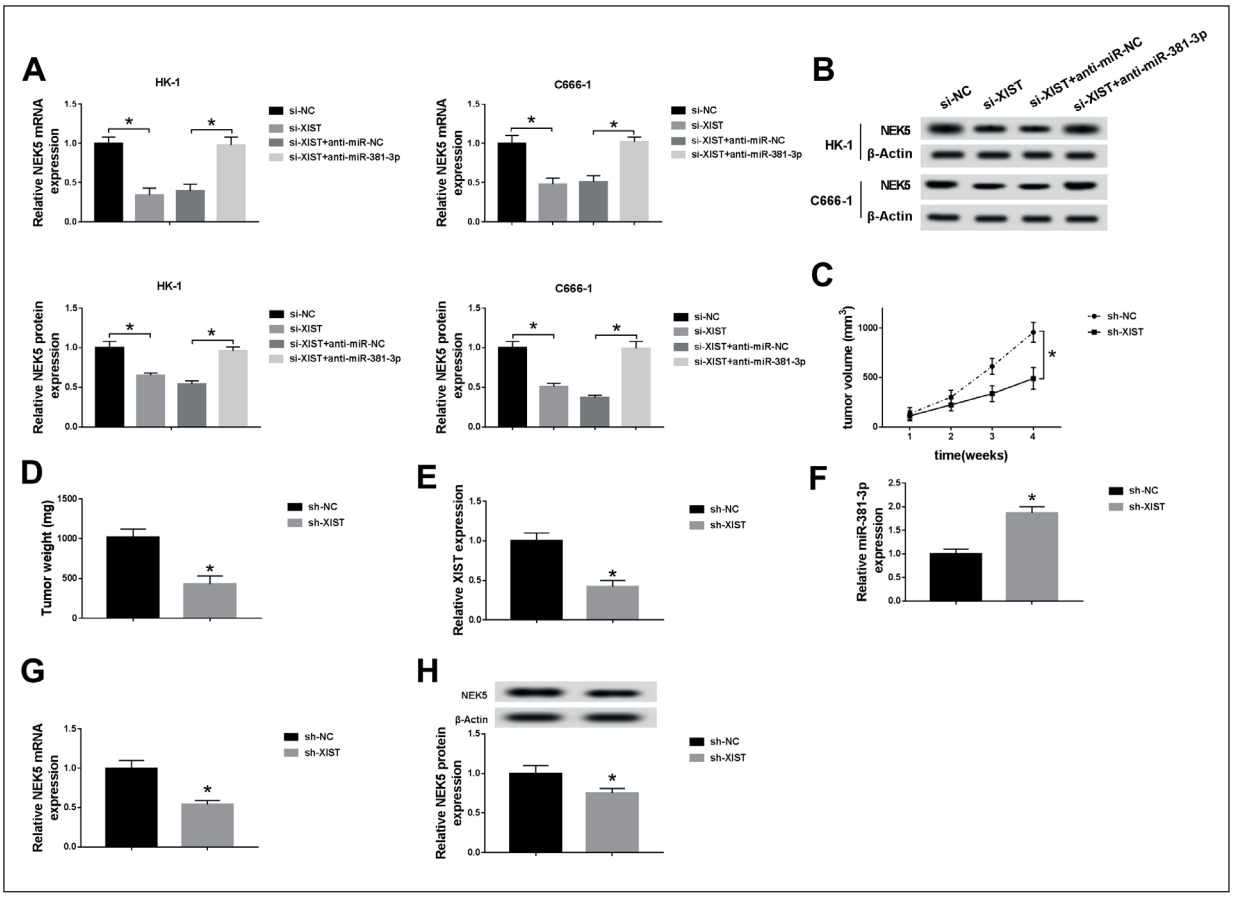

Figure 8. XIST served as a molecular sponge of miR-381-3p to regulate NEK5 expression. **A**-**B**, The mRNA and protein expression of NEK5 were examined in HK-1 and C666-1 cells transfected with si-NC, si-XIST, si-XIST + anti-miR-NC, or si-XIST + anti-miR-381-3p. **C**-**D**, HK-1 cells transfected with sh-NC or sh-XIST were injected subcutaneously into nude mice, tumor volume and weight were measured. **E**-**G**, The expression of XIST, miR-381-3p and NEK5 was measured by qRT-PCR in resected tumor tissues. **H**, The protein level of NEK5 was detected using Western blot analysis in resected tumor tissues. *$p<0.05$.

ifested that NEK5 expression was overexpressed in breast cancer tissues and linked to tumor progression and poor overall prognosis. Furthermore, Nikitina et al[42] proved that NEK5 expression was enhanced in prostate cancer tissues. Nevertheless, the role of NEK5 in NPC progression has not been investigated. In our study, the data displayed that NEK5 was expressed at a high level in NPC tissues and cells, suggesting that NEK5 served as a tumor promoter in NPC. Moreover, the interference of NEK5 suppressed hypoxia-induced glycolysis and metastasis and could reverse the pro-tumor role of miR-381-3p knockdown in hypoxia-induced cells. Furthermore, we uncovered that NEK5 was positively regulated by XIST and negatively regulated by miR-381-3p. Likewise, *in vivo* experiments displayed that silencing XIST restrained tumor growth *via* enhancing miR-381-3p and reducing NEK5. In a word, these findings disclosed that XIST acted as a molecular sponge of miR-381-3p to modulate NEK5 expression.

Conclusions

These findings displayed that XIST was upregulated in NPC and hypoxia-induced NPC cells. Knockdown of XIST inhibited hypoxia-induced glycolysis and metastasis in NPC cells by upregulating miR-381-3p and downregulating NEK5 expression. These data provided a novel mechanism for understanding NPC progression under hypoxic condition and might offer a potential therapeutic strategy for NPC.

Conflict of Interest

The Authors declare that they have no conflict of interests.

References

1) Torre LA, Bray F, Siegel RL, Ferlay J, Lortet-tieulent J, Jemal A. Global cancer statistics, 2012. CA Cancer J Clin 2015; 65: 87-108.
2) Wei KR, Zheng RS, Zhang SW, Liang ZH, Ou ZX, Chen WQ. Nasopharyngeal carcinoma incidence and mortality in China in 2010. Chin J Cancer 2014; 32: 381-387.
3) Colaco RJ, Betts G, Donne A, Swindell R, Yap BK, Sykes AJ, Slevin NJ, Homer JJ, Lee LW. Nasopharyngeal carcinoma: a retrospective review of demographics, treatment and patient outcome in a single centre. Clin Oncol (R Coll Radiol) 2013; 25: 171-177.
4) Eales KL, Hollinshead KE, Tennant DA. Hypoxia and metabolic adaptation of cancer cells. Oncogenesis 2016; 5: e190.
5) Giatromanolaki A, Sivridis E, Arelaki S, Koukourakis MI. Expression of enzymes related to glucose metabolism in non-small cell lung cancer and prognosis. Exp Lung Res 2017; 43: 167-174.
6) Semenza GL. The hypoxic tumor microenvironment: a driving force for breast cancer progression. Biochim Biophys Acta 2016; 1863: 382-391.
7) Huang R, Zong X. Aberrant cancer metabolism in epithelial-mesenchymal transition and cancer metastasis: mechanisms in cancer progression. Crit Rev Oncol Hematol 2017; 115: 13-22.
8) Wilusz JE, Hongjae S, Spector DL. Long noncoding RNAs: functional surprises from the RNA world. Genes Dev 2009; 23: 1494-1504.
9) Yang QQ, Deng YF. Genome-wide analysis of long non-coding RNA in primary nasopharyngeal carcinoma by microarray. Histopathology 2015; 66: 1022-1030.
10) Li L, Gu M, You B, Shi S, Shan Y, Bao L, You Y. Long non-coding RNA ROR promotes proliferation, migration and chemoresistance of nasopharyngeal carcinoma. Cancer Sci 2016; 107: 1215-1222.
11) Song P, Yin SC. Long non-coding RNA EWSAT1 promotes human nasopharyngeal carcinoma cell growth in vitro by targeting miR-326/-330-5p. Aging (Albany NY) 2016; 8: 2948-2960.
12) Chen DL, Ju HQ, Lu YX, Chen LZ, Zeng ZL, Zhang DS, Luo HY, Wang F, Qiu MZ, Wang DS, Xu DZ, Zhou ZW, Pelicano H, Huang P, Xie D, Wang FH, Li YH, Xu RH. Long non-coding RNA XIST regulates gastric cancer progression by acting as a molecular sponge of miR-101 to modulate EZH2 expression. J Exp Clin Cancer Res 2016; 35: 142.
13) Zhuang LK, Yang YT, Ma X, Han B, Wang ZS, Zhao QY, Wu LQ, Qu ZQ. MicroRNA-92b promotes hepatocellular carcinoma progression by targeting Smad7 and is mediated by long non-coding RNA XIST. Cell Death Dis 2016; 7: e2203.
14) Fang J, Sun CC, Gong C. Long noncoding RNA XIST acts as an oncogene in non-small cell lung cancer by epigenetically repressing KLF2 expression. Biochem Biophys Res Commun 2016; 478: 811-817.
15) Song P, Ye LF, Zhang C, Peng T, Zhou XH. Long non-coding RNA XIST exerts oncogenic functions in human nasopharyngeal carcinoma by targeting miR-34a-5p. Gene 2016; 592: 8-14.
16) Salmena L, Poliseno L, Tay Y, Kats L, Pandolfi PP. A ceRNA hypothesis: the Rosetta stone of a hidden RNA language? Cell 2011; 146: 353-358.
17) Calin GA, Croce CM. MicroRNA signatures in human cancers. Nat Rev Cancer 2006; 6: 857.
18) Yang X, Ruan H, Hu X, Cao A, Song L. miR-381-3p suppresses the proliferation of oral squamous cell carcinoma cells by directly targeting FGFR2. Am J Cancer Res 2017; 7: 913-922.
19) Shang A, Zhou C, Bian G, Chen W, Lu W, Wang W, Li D. miR-381-3p restrains cervical cancer pro-

gression by downregulating FGF7. J Cell Biochem 2019; 120: 778-789.

20) Kong W, Yang L, Li PP, Kong QQ, Wang HY, Han GX, Wang QB. MiR-381-3p inhibits proliferation, migration and invasion by targeting LRP6 in papillary thyroid carcinoma. Eur Rev Med Pharmacol Sci 2018; 22: 3804-3811.

21) Melo Hanchuk TD, Papa PF, La Guardia PG, Vercesi AE, Kobarg J. Nek5 interacts with mitochondrial proteins and interferes negatively in mitochondrial mediated cell death and respiration. Cell Signal 2015; 27: 1168-1177.

22) Shimizu K, Sawasaki T. Nek5, a novel substrate for caspase-3, promotes skeletal muscle differentiation by up-regulating caspase activity. FEBS Lett 2013; 587: 2219-2225.

23) Prosser SL, Sahota NK, Pelletier L, Morrison CG, Fry AM. Nek5 promotes centrosome integrity in interphase and loss of centrosome cohesion in mitosis. J Cell Biol 2015; 209: 339-348.

24) Marchio I, Pouyssegur J. Hypoxia, cancer metabolism and the therapeutic benefit of targeting lactate/H(+) symporters. J Mol Med (Berl) 2016; 94: 155-171.

25) Mathupala SP, Rempel A, Pedersen PL. Aberrant glycolytic metabolism of cancer cells: a remarkable coordination of genetic, transcriptional, post-translational, and mutational events that lead to a critical role for type II hexokinase. J Bioenerg Biomembr 1997; 29: 339-343.

26) Jin B, Jin H, Wu HB, Xu JJ, Li B. Long non-coding RNA SNHG15 promotes CDK14 expression via miR-486 to accelerate non-small cell lung cancer cells progression and metastasis. J Cell Physiol 2018; 233: 7164-7172.

27) Bartel DP. MicroRNAs: target recognition and regulatory functions. Cell 2009; 136: 215-233.

28) Mucaj V, Shay JE, Simon MC. Effects of hypoxia and HIFs on cancer metabolism. Int J Hematol 2012; 95: 464-470.

29) Shi J, Wang H, Feng W, Huang S, An J, Qiu Y, Wu K. Long non-coding RNA HOTTIP promotes hypoxia-induced glycolysis through targeting miR-615-3p/HMGB3 axis in non-small cell lung cancer cells. Eur J Pharmacol 2019; 862: 172615.

30) Kong YG, Cui M, Chen SM, Xu Y, Xu Y, Tao ZZ. LncRNA-LINC00460 facilitates nasopharyngeal carcinoma tumorigenesis through sponging miR-149-5p to up-regulate IL6. Gene 2018; 639: 77-84.

31) Nie GH, Li Z, Duan HF, Luo L, Hu HY, Yang WQ, Nie LP, Zhu RF, Chen XF, Zhang W. lncRNA C22orf32-1 contributes to the tumorigenesis of nasopharyngeal carcinoma. Oncol Lett 2017; 13: 4487-4492.

32) Wang Z, Yuan J, Li L, Yang Y, Xu X, Wang Y. Long non-coding RNA XIST exerts oncogenic functions in human glioma by targeting miR-137. Am J Transl Res 2017; 9: 1845-1855.

33) Fang J, Sun CC, Gong C. Long noncoding RNA XIST acts as an oncogene in non-small cell lung cancer by epigenetically repressing KLF2 expression. Biochem Biophys Res Commun 2016; 478: 811-817.

34) Song P, Ye LF, Zhang C, Peng T, Zhou XH. Long non-coding RNA XIST exerts oncogenic functions in human nasopharyngeal carcinoma by targeting miR-34a-5p. Gene 2016; 592: 8-14.

35) Cheng Q, Xu X, Jiang H, Xu L, Li Q. Knockdown of long non-coding RNA XIST suppresses nasopharyngeal carcinoma progression by activating miR-491-5p. J Cell Biochem 2018; 119: 3936-3944.

36) Koukourakis MI, Giatromanolaki A, Simopoulos C, Simopoulos C, Polychronidis A, Sivridis E. Lactate dehydrogenase 5 (LDH5) relates to up-regulated hypoxia inducible factor pathway and metastasis in colorectal cancer. Clin Exp Metastasis 2005; 22: 25-30.

37) Zhang LF, Lou JT, Lu MH, Gao C, Zhao S, Li B, Liang S, Li Y, Li D, Liu MF. Suppression of miR-199a maturation by HuR is crucial for hypoxia-induced glycolytic switch in hepatocellular carcinoma. EMBO J 2015; 34: 2671-2685.

38) Militello G, Weirick T, John D, Doring C, Dimmeler S, Uchida S. Screening and validation of lncRNAs and circRNAs as miRNA sponges. Brief Bioinform 2017; 18: 780-788.

39) Momen-Heravi F, Bala S. Emerging role of non-coding RNA in oral cancer. Cell Signal 2018; 42: 134-143.

40) Wu M, Fan B, Guo Q, Li Y, Chen R, Lv N, Diao Y, Luo Y. Knockdown of SETDB1 inhibits breast cancer progression by miR-381-3p-related regulation. Biol Res 2018; 51: 39.

41) Li YY, Guo L, Li H, Li J, Dong F, Yi ZY, Ouyang YC, Hou Y, Wang ZB, Sun QY, Lu SS, Han Z. NEK5 regulates cell cycle progression during mouse oocyte maturation and preimplantation embryonic development. Mol Reprod Dev 2019; 86: 1189-1198.

42) Nikitina AS, Sharova EI, Danilenko SA, Butusova TB, Vasiliev AO, Govorov AV, Prilepskaya EA, Pushkar DY, Kostryukova ES. Novel RNA biomarkers of prostate cancer revealed by RNA-seq analysis of formalin-fixed samples obtained from Russian patients. Oncotarget 2017; 8: 32990-33001.